Fractal interfaces and product generation in the two dimensional mixing layer

By Javier Jiménez[1] AND Carlos Martel[2]

The dependence of product generation on Péclet and Reynolds numbers in a numerically simulated, reacting, two dimensional, temporally growing mixing layer is related theoretically to the fractal dimension of the passive scalar interfaces. This relation is verified using product generation measurements and dimensions derived from a standard box counting technique. A transition from a low initial dimension to a higher one of approximately 5/3 is identified and shown to be associated to the kinematic distortion on the flow field during the first pairing interaction. It is suggested that the structures responsible for this transition are non-deterministic, non-random, inhomogeneous fractals. Only the large scales are involved. No further transitions, either in the spectra of the vorticity field or in the mixing behavior, are found for Reynolds numbers up to 90 000.

Introduction

It has been realized for some time that smooth velocity fields can generate very complicated advective scalar distributions (Aref, 1984) and, in particular, that initially smooth interfaces can become very convoluted. In fact, even if such an interface remains technically rectifiable for any finite amount of time, its geometry becomes more and more complicated, and we shall give below simple examples in which it develops fractal properties over a wide range of length scales. When seen at those scales, its area increases substantially, and if the interface separates two fluids that are to be mixed by molecular diffusion, the stretching results in a enhancement of the mixing efficiency. A convenient measure of the complication of the interface and, indirectly, of its area increase is its fractal dimension (Mandelbrot, 1982).

We will show here that in the *two dimensional* mixing layer, a transition occurs at the location of the first pairing interaction, resulting in the development of a fractal range in the geometry of scalar interfaces with dimensions of the order of 5/3. We will also show that this fractal behavior can be related to the scaling properties of the total amount of product with Péclet number.

Assume a two dimensional situation in which the interface separating two immiscible fluids can be described by a line with a fractal dimension, F. Diffusion will "blur" the interface and generate a mixed region in the form of a strip centered around the original line whose width will, from dimensional considerations, be proportionally to $W = D^{1/2}$, where D is the molecular diffusivity. This is true both for flows in which strain is not important, in which case the width grows in time as

1 Center for Turbulence Research and Universidad Politécnica Madrid

2 Universidad Politécnica Madrid

$W = (Dt)^{1/2}$, and for those dominated by interface straining, in which the mixed region attains a steady width $W = (D/\gamma)^{1/2}$ where γ is the strain.

Directly from the definition of the fractal dimension (Mandelbrot, 1982), if a fractal line is covered with elements of diameter, W, the number of elements needed for the covering is proportional to $N \sim W^{-F}$, and the line length seen at that scale is $L(W) \approx NW \sim W^{1-F}$. In the same way, the area of the strip formed by all the covering elements which, in the case of the diffusive interface is proportional to the area occupied by the mixed fluid, is $S \approx N W^2 \sim W^{2-F}$. Note that since for non intersecting fractal lines in a plane, $1 < F \leq 2$, the length of a fractal interface will always diverge as we sample it at increasingly smaller scales, but the strip area will vanish in the limit (except for the surface filling case, $F = 2$). If we now go back to the problem of mixing and repeat the same mixing experiment with all dimensions constant but with different diffusivities, the area of the mixed strip and, therefore, the amount of mixed fluid will be proportional to

$$S \sim D^{1-F/2} \sim Pe^{F/2-1}, \tag{1}$$

where $Pe = UL/D$ is the Péclet number. This equation contains the "practical" implication of the fractal dimension of the fluid interface, and we will use it in the next section to estimate F from product generation data. An equivalent formulation exists for three dimensional situations in which the exponent in equation (1) is replaced by $(F-3)/2$.

Note that if we compare two flows with interfaces having different fractal dimensions, nothing in equation (1) guarantees that for a given Pe, the amount of mixing will increase with fractal dimension. However, if the diffusivity is reduced, the amount of mixing will decrease more slowly for the flow with higher F, and for some sufficiently high Pe, the more highly fractal flow will always generate more mixing. The assumption in this argument is that the immiscible interface itself is independent of Pe, either because the velocity field is kept constant among different experiments, as in those cases in which Pe is increased by varying only the Schmidt number, Sc, or because the changes in the velocity field are small and irrelevant to the global geometry of the interface. This latter seems to be the case in the two dimensional flows described here but probably does not apply to the mixing transition observed in three dimensional layers (Konrad, 1977, Breidenthal, 1981), in which the flow itself becomes considerably more complex as Re increase (Moser and Rogers, 1990). In those cases, it is still possible to use the arguments given above to explain the variation of the mixing efficiency with Sc, but the discussion of the Reynolds number dependence must include considerations of the flow dynamics.

In this paper, we describe some numerical experiments on the generation of product by a simple chemical reaction in a two dimensional, incompressible, temporally growing, mixing layer. The amount of product is controlled by diffusion, and it will be taken as representative of the amount of mixing and used as such in equation (1). The initial conditions are held constant as the Reynolds and Péclet numbers are changed both together and independently, and the variation in product generation is used to deduce the fractal dimension of a theoretical interface separating

two immiscible species. These fractal dimensions are then compared with those obtained by a purely geometrical analysis of the interface. The numerical code and the experimental procedure are discussed briefly in the next section, and the results are then presented and discussed.

Experimental arrangements

The numerical code is a full Navier-Stokes simulator, developed at the Universidad Politécnica in Madrid using the vorticity-stream function formulation in conservative form, and includes the transport equation for a passive scalar. It uses a Fourier spectral representation in the streamwise (x) direction and a fourth order (Padé) finite difference scheme in the transverse (y) coordinate. The grid is mapped to infinity, and the nonlinear terms are computed using a fully de-aliased collocation scheme. Typical grids use 512 Fourier modes (341 after de-aliasing) and 400 transverse points (1024×800 for $Re = 1600$). The code solves the initial value problem, starting with a initial velocity distribution, $u(y) = \tanh(y)$. This profile is perturbed initially with a small sinusoidal transverse deformation of amplitude, $\Delta y \approx 0.1$ and wavelength, $\alpha = 0.4$, which is close to the most amplified one for the initial Kelvin Helmholtz instability. In most of the runs, the computational box contains four initial wavelengths, resulting in the formation of four primary eddies that later interact through pairing. To insure this, small subharmonic and sub-subharmonic components are added to the initial perturbation.

A dimensionless viscosity is defined in terms of a Reynolds number based on the half velocity difference across the layer and on half the initial vorticity thickness, $\delta_\omega = 2$. The initial distribution of the passive scalar is taken as $s = 0.5(1 + \tanh(y/L_s))$, and its evolution is controlled by a Schmidt number, Sc, related to Re and the Péclet numbers by $Pe = Sc\,Re$. In most cases, $Sc = 1$, but some tests were done with Schmidt numbers in the range 0.25 to 4. The evolution of the scalar is used to model the behavior of a fast binary chemical reaction, $A + B \rightarrow P$, between species A and B, each of which is initially assumed to be distributed uniformly in one stream. Later they diffuse through the mixing layer and react immediately. The parameter, L_s, determines the width of the initial mixed region and should ideally be as small as possible to approximate a sharp interface. Numerical limitations prevent this, and all our experiments have been done with $L_s = 0.3$. For the most unfavorable case of high Péclet number, the memory of this initial thickness seems to be lost by the flow before $t = 20$, approximately the time necessary for the formation of the primary Kelvin-Helmhotz eddies.

In the Burke-Schumann limit assumed here, given the local concentration of the scalar, s, the concentration of product, P, can be shown to be proportional to

$$P = 2s \quad \text{if} \quad s < 1/2, \qquad P = 2(1 - s) \quad \text{otherwise.}$$

With this normalization, the maximum product concentration is always locally equal to one, and the center of the product distribution follows the $s = 0.5$ isoline. The product thickness,

$$\delta_p = \int_0^{L_x} P\,dx/L_x, \tag{2}$$

is a good measure of the area occupied by the reaction product, and we will take it as a measure of the mixed fluid area to be used in computing the fractal dimension through the arguments leading to equation (1). L_x is the length of the computational box.

The temporal evolution of flow

Some typical time histories of the vorticity and momentum thickness are shown in figure 1. There are several bumps in the vorticity thickness evolution which mark the initial roll-up into vortex cores and two consecutive pairings. It is a property of temporal simulations that the time at which each pairing occurs can be controlled by varying the amplitudes of the initial subharmonic perturbations. These were chosen so as to reproduce as closely as possible the experimental observations in an unforced half jet (Jiménez, 1983). The evolution of the vorticity thickness is too irregular to be described by a linear growth rate, but a least square fit to the lines in figure 1a has a slope of 0.22, which is in reasonable agreement with the experimental growth rates for tripped shear layers. The evolution of the momentum thickness also shows bumps, although shallower, and its mean growth rate, 0.14 ± 0.02, is also approximately consistent with experiments. Later we will discuss briefly simulations in which the first and second pairings were purposely inhibited. In those cases, the vorticity thickness grows at the beginning as in the natural case but eventually levels off and oscillates about a fixed value.

Figure 2 shows the temporal evolution of the product thickness, which is much more linear and much less affected by the pairing. Its rate of growth is very dependent on Pe, decreasing with decreasing diffusivity. In fact, Pe, as opposed to Re, seems to be the controlling parameter in product generation. All the solid lines in figure 2 represent simulations with $Sc = 1$, while the dashed lines correspond to simulations at different Schmidt numbers. Those lines always correspond to the Péclet number to which they are closest, and the effect of Re seems to be slight. In particular, $Pe = 1600$ was run both at $Sc = 1$, and at $Re = 400$, $Sc = 4$. Also $Pe = 800$ and $Pe = 200$ were both run at $Re = 200$ and $Re = 800$. In all these cases, even if the Reynolds numbers were quite different and even if the vorticity fields shows appreciably more visual complication at the higher ones (see figure 3), the product thickness scales almost exclusively with Pe, with variations below 3% which, at the end of the run, even tend to be of the opposite sign to those at the earlier moments. This suggests that most of the interface is generated by the action of the large vortical structures which are relatively independent of Reynolds number instead of by the small scales, whose energy in this two dimensional flow is relatively small.

Note that these Re and Pe are actually quite high since they are referred to the initial state of the layer. In fact, when they are reduced to local quantities at the last stage in the simulation, $Re_\omega = \Delta U\, \delta_\omega / \nu$ is of the order of 90 000 for $Re = 1600$ (the fitted value, $\delta_\omega = 0.22t$, has been used for this reduction.)

Figure 4 contains enstrophy spectra for the highest Reynolds number simulation at different times. They are one dimensional (x) spectra and have been averaged

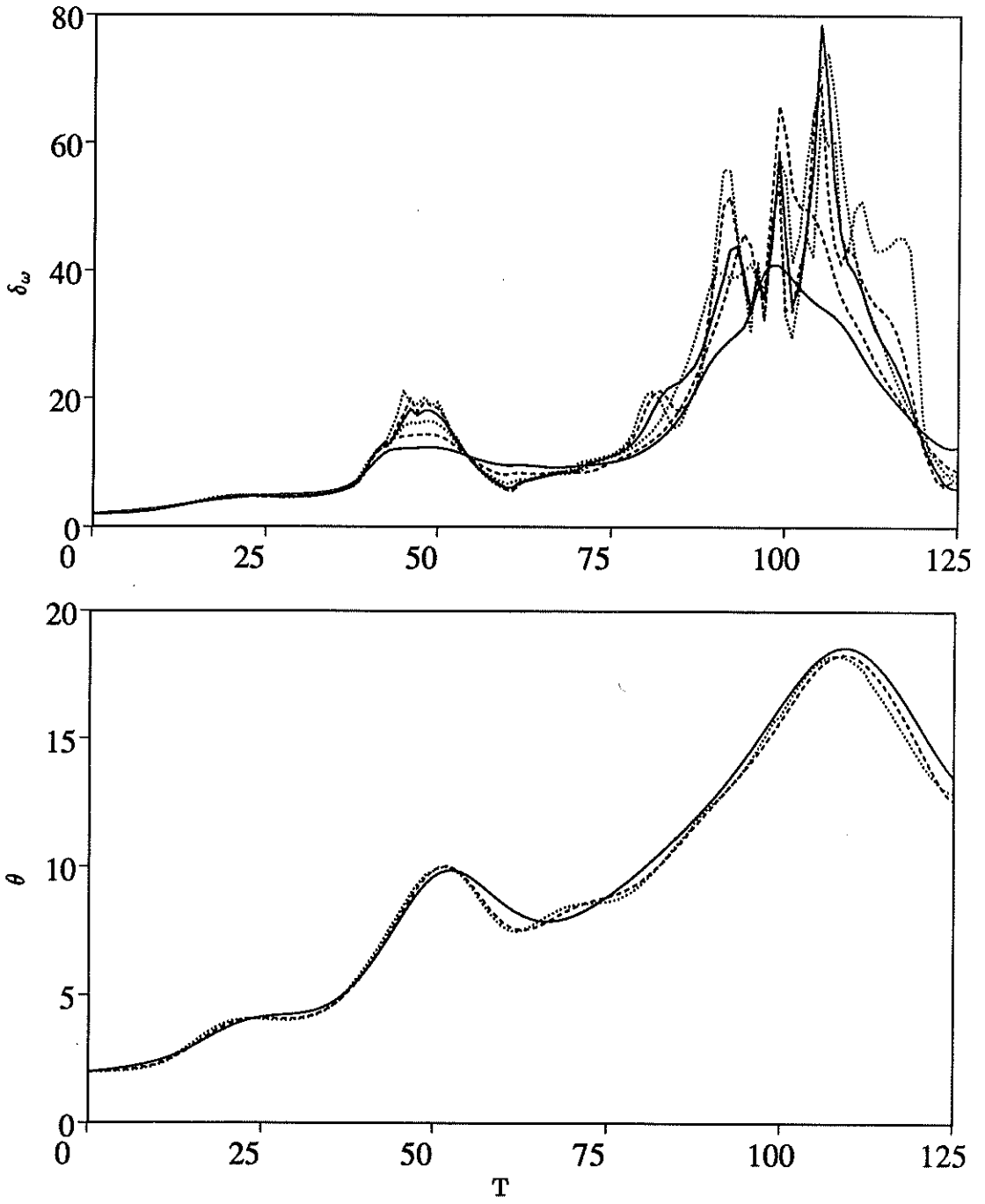

FIGURE 1. Time evolution of vorticity (top) and momentum thickness (bottom). For δ_ω, Re = 50, 100, 200, 400, 800, 1600, in order of increasing thickness during the first pairing. For the momentum thickness, Re = 100, 400, 1600.

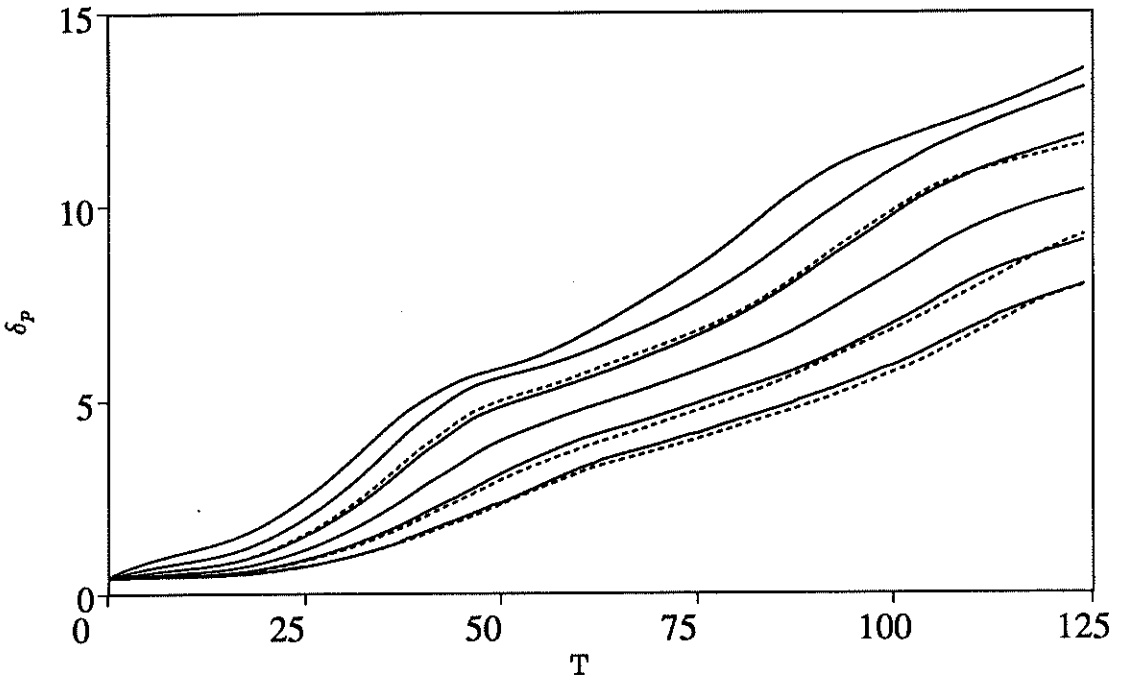

FIGURE 2. Time evolution of product thickness. Solid lines: $Re = Pe = 50$, 100, 200, 400, 800, 1600, in order of decreasing thickness. Dashed lines, also in order of decreasing thickness: $Re = 800$, $Pe = 200$; $Re = 200$, $Pe = 800$, and $Re = 400$, $Pe = 1600$. Note that histories with $Sc \neq 1$ cluster near equivalent Pe, independent of Re.

in each case over approximately the central 60% of the vorticity thickness. No normalization is introduced, and each spectrum should integrate to the averaged value of ω^2. A steep viscous range is always present, extending up to the maximum numerical wavenumber, ($\kappa = 10^2$). Approximately after the first pairing, ($t = 50$) an "inertial" range appears with an exponent slightly shallower than κ^{-2}, corresponding to an energy spectrum behavior, $E(\kappa) \sim \kappa^{-4}$, in good agreement with the results of Lesieur *et al.* (1988). It is interesting to note that the break between the two ranges is always close to $\kappa \approx 8 - 10$, corresponding to lengths of O(1), which are comparable to the smallest scales introduced by the initial conditions. Also, after the initial roll-up, the inertial range of the spectra moves uniformly to weaker energies, and there is never a tendency for a turbulent cascade to generate small scales in the same sense as in three dimensional flows. Correspondingly, the maximum vorticity stays bounded below its maximum initial value, $\omega = 1$, which is, of course, a consequence of the two dimensionality and incompressibility assumptions, and which contrasts sharply with the behavior of three dimensional flows, in which transition occurs through the generation of strong concentrated vortices through stretching, and through the appearance of scales much smaller that the pre-transition ones. As a consequence, this two dimensional flow suffers no "mixing

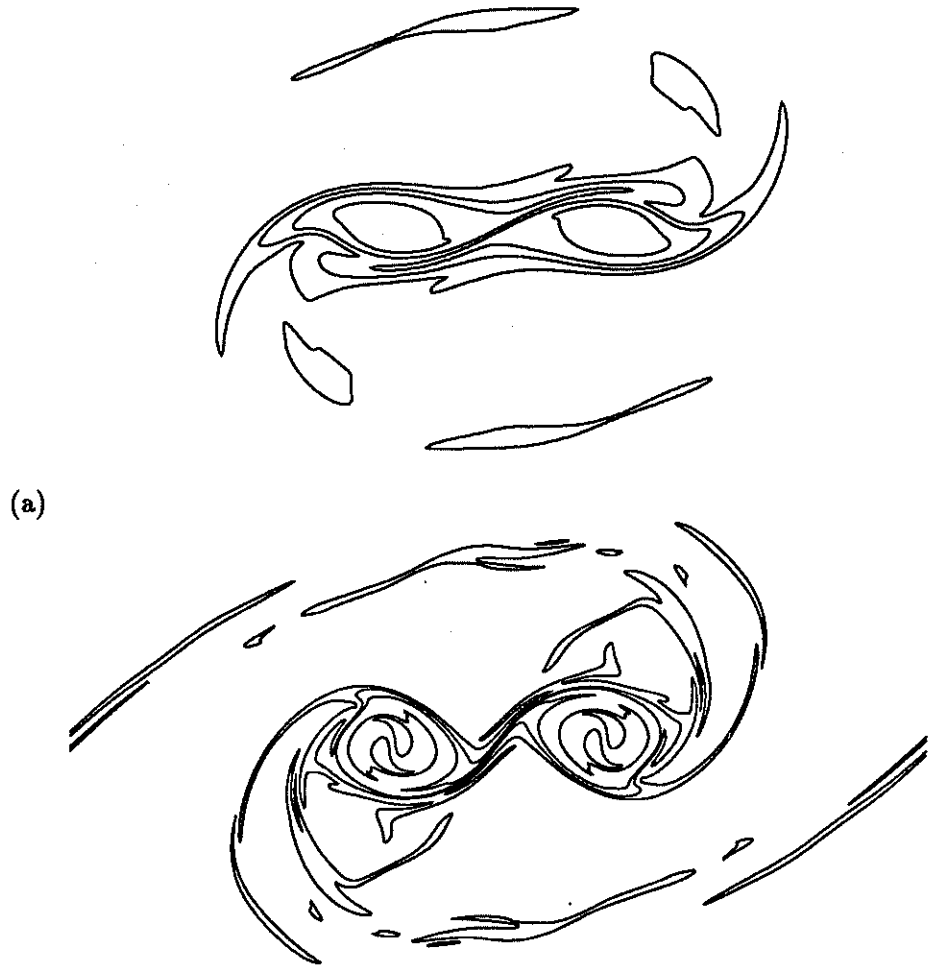

(a)

(b)

FIGURE 3. Vorticity maps for the flow at identical evolution stages, $t = 125$, after second pairing. (a) $Re = 400$, $Re_\omega = 2.2 \times 10^4$, (b): $Re = 1600$, $Re_\omega = 8.8 \times 10^4$. Isolines: $\omega = 0.1, 0.9\,(0.2)$.

transition" in the same sense as the three dimensional mixing layer.

In fact, figure 2 shows that the generation of product decreases uniformly with increasing Reynolds and Péclet numbers. A plot of δ_p against Pe is given in figure 5, where each line represents an instant in time for different Péclet numbers, and time increases upwards. Especially at the later times, a self similar range develops in which the product dependence with Pe can be well approximated by a power law. The slopes of these lines are the exponents discussed in equation (1) and can be related directly to the dimension of the fractal interfaces. At the last stages of the evolution of the layer where the self similarity holds over a wide range of scales, this dimension has a direct geometric meaning, while at the initial stages it should

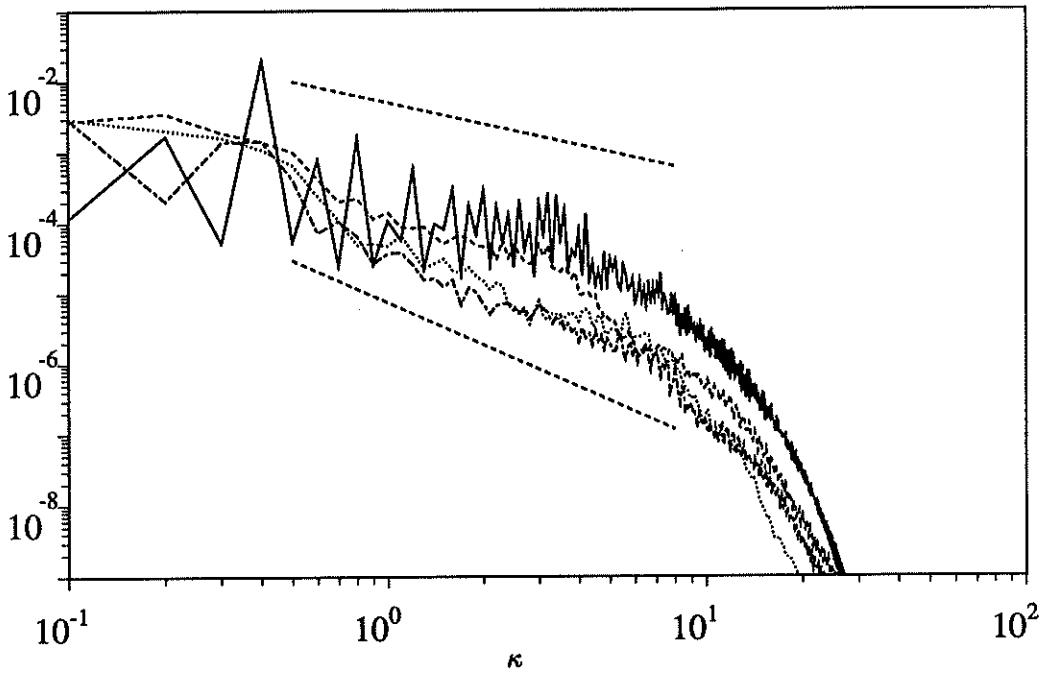

FIGURE 4. Enstrophy (ω^2) spectra *vs.* wavenumber, κ. Solid line: $t = 25$, chain-dashed: 75, dotted: 100, dashed: 125. Lower straight line: κ^{-2}. Upper: κ^{-1}.

be understood more as an averaged value over the range of scales sampled by the thickness of the diffusion layers. The time evolution of F computed in this way is given by the open circles in figure 6. It is clear that a transition occurs near $t = 50$, which corresponds to immediately after the first pairing interaction. The second pairing near $t = 100$ also induces a slight increase in F, but a much weaker one, and the dimension seems to asymptote to a value close to 5/3. Before $t = 20$, the time of initial roll-up, the measurement of F is prevented by the effect of the finite thickness of the initial condition for s, but the dimension has to approach that of a smooth line ($F = 1$) for short times. The two other sets of open symbols in figure 6 refer to two different sets of runs in one of which the second pairing was inhibited, while in the other both pairings were prevented. It is clear that the effect of the second pairing is small but that the absence of the first pairing prevents completely the appearance of the fractal transition. The closed symbols in this figure correspond to fractal dimensions computed directly from the interface geometry and will be discussed below.

The geometry of the product distribution

Before we are ready to identify the quantity, F, obtained in the last section with the fractal dimension of the immiscible interface, we need to prove that it coincides with the dimension derived from standard geometric methods, and we have to clarify over which range of length scales the implied power law is valid. As explained in

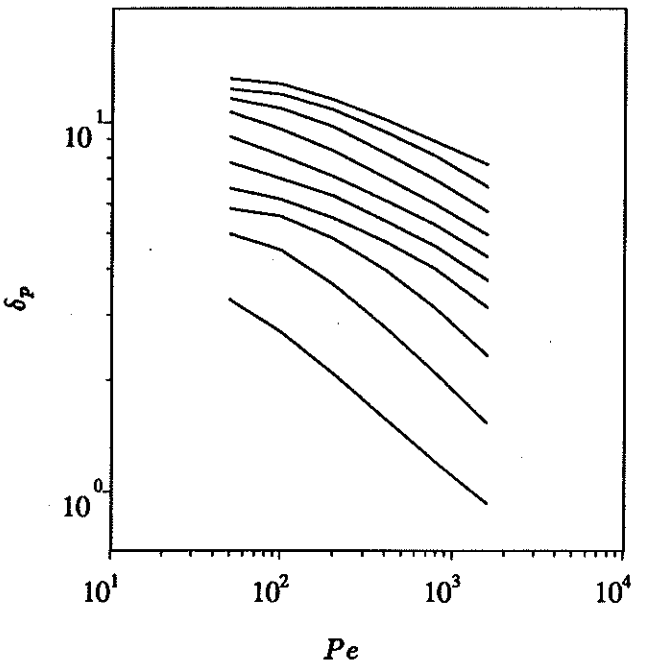

FIGURE 5. Variation of product thickness with Péclet number for different times. $t = 30$, 120, (10), increasing upwards. Data as in figure 2, $Sc = 1$.

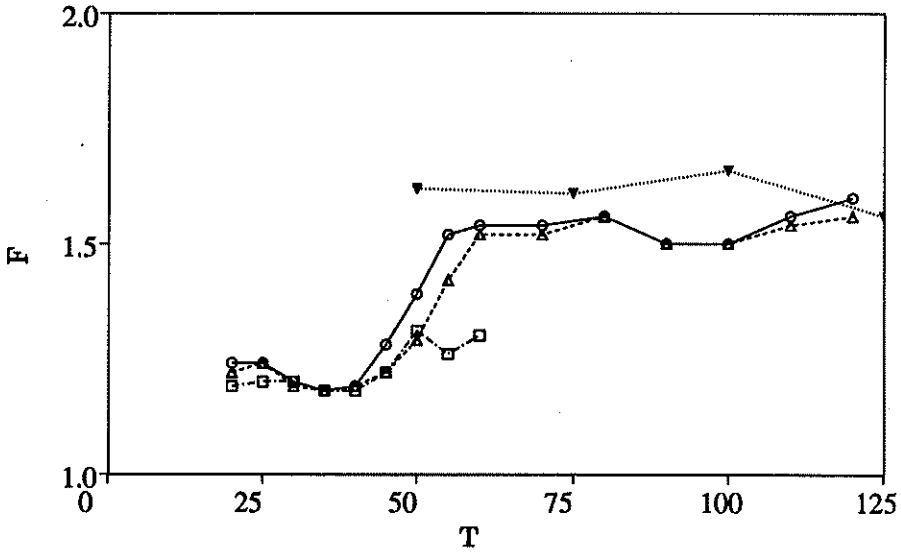

FIGURE 6. Fractal dimension of the interface, computed from figure 5, and from other similar data sets. ○: Natural layer, two pairings; △: Second pairing inhibited; □: All pairings inhibited. Closed triangles: Fractal dimensions obtained from direct box counting.

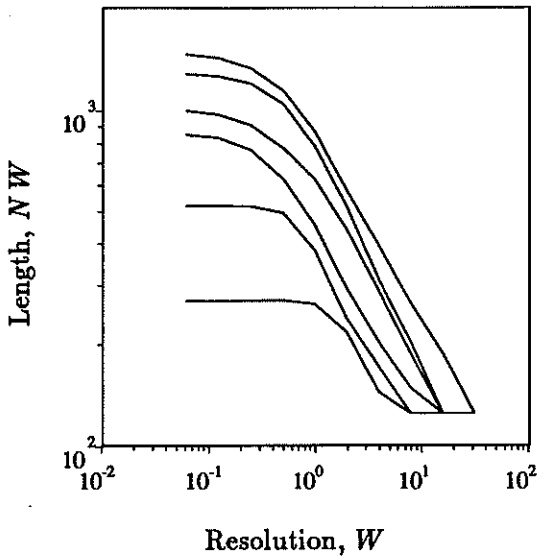

FIGURE 7. Length-resolution fractal diagrams for the $s = 0.5$ isoline for the $Re = Pe = 1600$ simulation. Times: 25, 37.5, 50, 75, 100, 125, moving upwards.

the introduction, the simplest way of measuring the fractal dimension of a line is to count the number, $N(W)$, of elements of uniform size, W, that are needed to cover it. Directly from the definition, the dimension is then given by the exponent in the relation

$$N \sim W^{-F}. \tag{3}$$

The easiest way to do this is to cover the line with a square grid of a small pitch and to plot how the number of grid cells crossed by the line changes as the pitch of the grid is successively doubled. The result for the $s = 0.5$ isoline of the convected scalar for the simulation at $Re = Pe = 1600$ is given in figure 7. That isoline corresponds to the location of an infinitely thin diffusion flame for a reaction with unit stoichiometric ratio. It is seen that initially the fractal range, if it exists at all, is very short but that eventually a substantial self similar range develops, spanning scales almost over two orders of magnitude. The corresponding fractal dimensions are represented in figure 6 by closed symbols and agree reasonably well with those obtained from the product generation. Note that the quantity plotted in figure 7 is the product, $N\,W$, proportional to the line length, and that the horizontal segments on the upper left hand part of the plot correspond to a range of scales for which the interface can be considered to be smooth and to have a well defined length. The horizontal segments at the bottom of the graph mark the opposite limit in which the whole mixing layer appears as a "thick" line, (2×1 cells across).

The extent of the fractal range

It is interesting to estimate the range of scales that can be considered fractal and

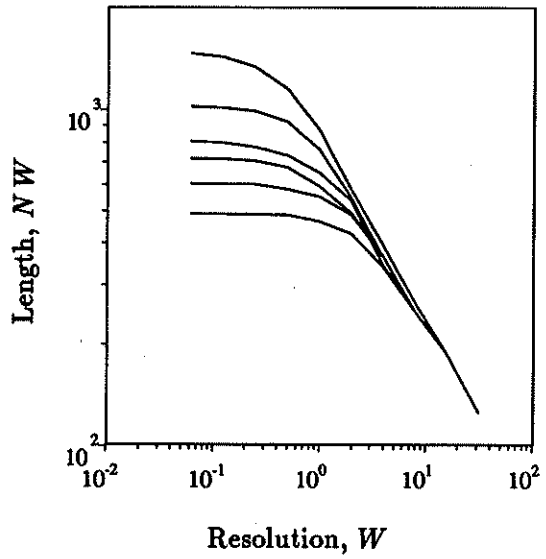

FIGURE 8. Length-resolution fractal diagrams for the $s = 0.5$ isoline for $t = 125$. $Pe = Re = 50, 100, 200, 400, 800, 1600$, moving upwards.

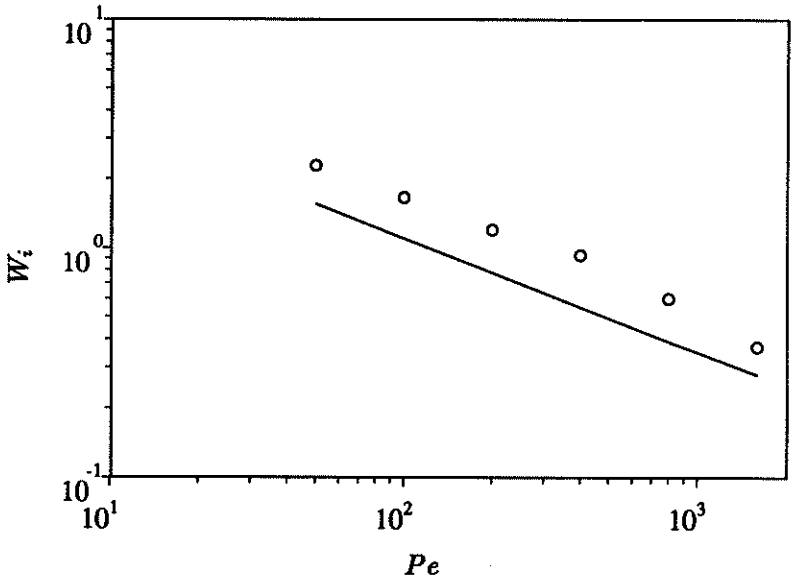

FIGURE 9. Inner cut-off scale for the fractal range, as function of Pe number. $t = 125$. Straight line is estimation of minimum diffusion scale, see text.

to compare it with the extent of the self similar power law ranges observed in figure 7. It is clear that even in the absence of diffusion, there are minimum and maximum length scales beyond which the fractal assumption fails. The solutions of the two dimensional Navier Stokes equations are smooth (for finite Reynolds number and smooth initial conditions), and any smooth material line of finite length is deformed into lines of finite length. Since we have shown above that fractal lines are not rectifiable, an interface cannot become strictly fractal in a finite time, and there will always be a minimum scale below which the interface is smooth. It is possible, however, for this inner scale to be a decreasing function of time and for the interface to become a true self similar fractal in the asymptotic limit of infinite time.

Consider the simple model of a initially straight interface being rolled into a tight spiral around a potential vortex with an inner core of radius, ρ, and total circulation, Γ. This is, in fact, a good model for the initial phase of interface creation in the mixing layer, and it can be shown to lead to a fractal dimension of 4/3 (Jiménez & Martel, 1990). The source of the infinite length of this spiral is the infinite number of turns that eventually appear as the interface is wound around the inner core, and the inner scale of the fractal range can be identified as the distance between consecutive turns just outside the rotational core. It can easily be shown by direct calculation that this distance decreases asymptotically for large times as

$$W_i = \frac{\Delta r}{\rho} = \frac{t_\Gamma}{2t}, \qquad t_\Gamma = \frac{(2\pi\rho)^2}{\Gamma}, \tag{4}$$

The time scale, t_Γ, is the vortex turnover time measured at the edge of the inner core. In actual shear layers, this process is interrupted by the pairing and by viscous diffusion, but it probably explains the mild fractal properties of the interface in the early layer, which are apparent in figure 6 as the $F \approx 1.3$ plateau of the product generation dimension before the first pairing.

In fact, if we approximate the initial conditions as a layer of uniform vorticity and assume that it rearranges itself into uniform vortex cores without appreciable entrainment of irrotational fluid, we can estimate the radii of the initial cores as $\rho = (\delta_{\omega 0}\lambda_0/\pi)^{1/2}$, and their circulation as $\Gamma = \Delta U\,\lambda_0$, where $\delta_{\omega 0}$ is the initial vorticity thickness and λ_0 is the wavelength of the initial instability. The minimum length scale can then be written as $W_i = 2\pi\delta_{\omega 0}^2/\Delta U\,t$ which, in the units of our simulation, is just $W_i = 4\pi/t$. For the two curves in figure 6 which belong to this initial phase and taking into account that the initial roll-up occurs at $t \approx 20$, the result is $W_i = 2.5$ at $t = 25$ $(t - t_0 \approx 5)$, and $W_i = 0.7$ at $t = 37.5$. These values are in reasonable agreement with the location of the upper "corners" which mark in both curves the transition between the fractal behavior at large scales and the small scale smooth limit. This agreement suggests that the creation of interface in this initial phase is not limited by diffusion at the Péclet numbers of the simulation.

That this is not always the case can be seen in figure 8, which displays the behavior of the fractal diagram at $t = 125$ for different Péclet numbers. It is clear that the fractal range grows with increasing Pe. Let us define the location of the small scale cut-off as the point where the straight line defining the fractal range in the log-log

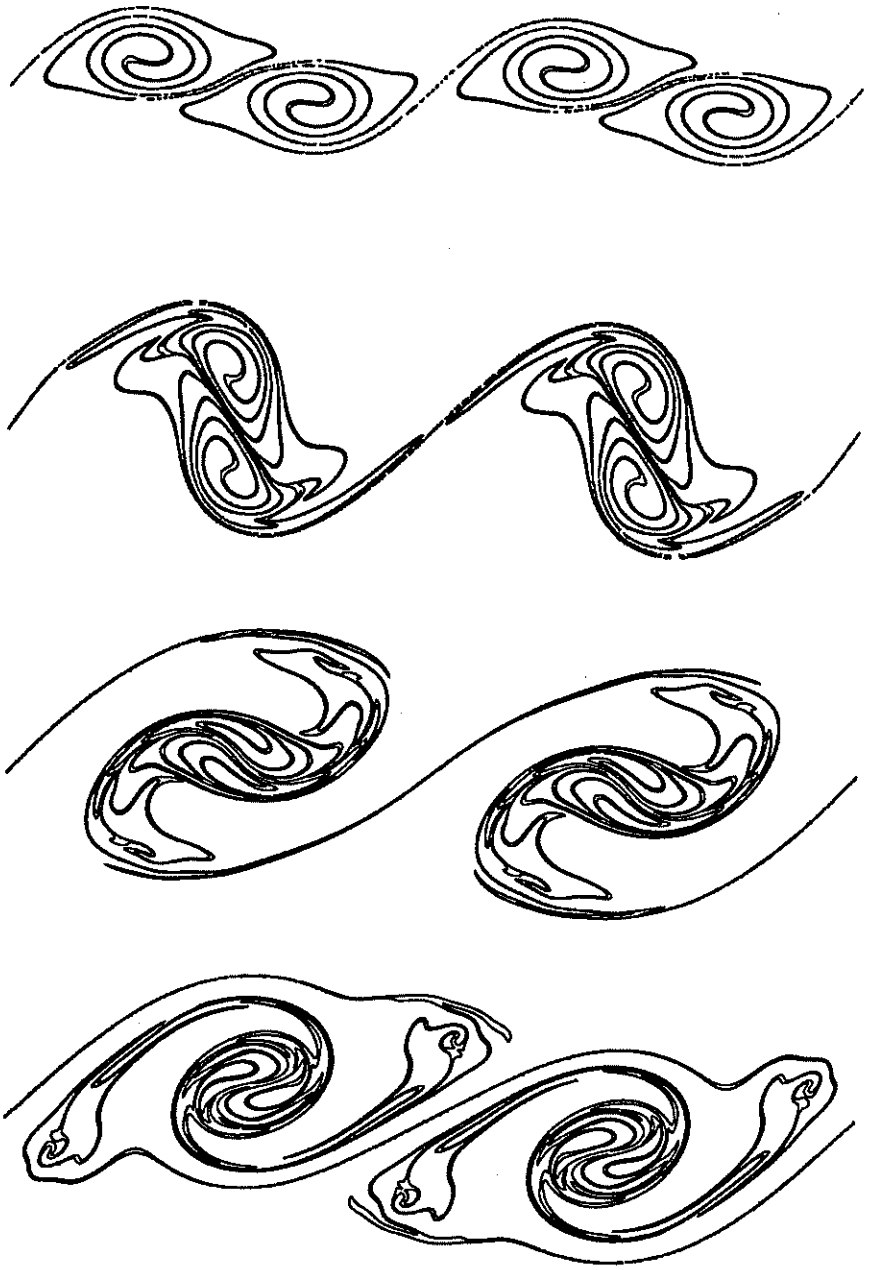

FIGURE 10. Product concentration maps during the first pairing. Time, top to bottom: $t = 37.5, 50, 62.5, 75$. $Re = Pe = 1600$. Isoline: $P = 0.8$ (equivalent to $s = 0.4, 0.6$). Note how initial spirals are deformed and stretched by pairing, especially in outer parts.

plot intersects the horizontal line marking the asymptotic value of the line length for small scales. The variation with Pe of the length scale corresponding to this point is given in figure 9, and scales quite closely with $Pe^{-1/2}$, suggesting that it is diffusion limited. In fact, it is of the same order of magnitude as the Batchelor scale for the mixing at that particular time, which can be estimated by noting that a diffusive interface in a strain $v = -\gamma y$ reaches an equilibrium thickness $\delta_\gamma = (2\pi/Pe\,\gamma)^{1/2}$. The maximum strain in a shear layer, modeled as a row of compact vortices, is of the order of $\gamma = \pi\,\Delta u/2\lambda$, where λ is the distance between consecutive vortices, and the equilibrium thickness becomes for the simulation corresponding to figure 9 $\delta_\gamma = (4\lambda/Pe\,\Delta U)^{-1/2} \approx 11\,Pe^{-1/2}$. This is the line drawn in figure 9 and agrees with the measured data not only in slope but also in order of magnitude.

These last estimates prove that, contrary to the situation during the early stages of roll-up, the generation of interface at these later stages and at this particular Péclet number is limited by molecular diffusion, and that simulations at higher Péclet numbers will reveal still more interface at the smaller scales.

The source of these small scales can be seen in figure 10, which shows the evolution of the interface through the first pairing. After roll-up, the interface forms tight spirals similar to those described previously, but during the pairing, these spirals are stretched, in part into elongated ellipses near the centers, but especially into long filamentary stacks in their outer parts, whose fractal character derives from the close proximity of successive leaves. Since area is conserved during the deformation, the distance between two leaves originating from the deformation of spiral turns of radius, R, and initially separated by a distance, W_R, becomes of the order of $W_L = W_R R/L$, where L is the length of the strip into which the initial circle is deformed. If we take this length to be of the order of the distance between eddies after pairing and the initial radius to be of the order of the vorticity thickness before pairing, the reduction in the minimum length scales imposed by the kinematics during pairing is roughly one decade. In our simulations, that will make it $W_i \approx 0.05$ after pairing, well below the resolution imposed by the diffusion scale which, as computed above, is $\delta_\gamma \approx 0.4$ for our $Pe = 1600$ case. It can be shown (Jiménez & Martel, 1990) that the appearance of these stacks leads to a fractal dimension of 5/3, and they are in all probability responsible for the fractal behavior of the interface in the late evolution of the layer.

Discussion

We have measured the change in time of the fractal dimension of an ideal interface in a two dimensional mixing layer, and we have related it to the scaling properties of product generation with Péclet number. We have also shown that this scaling holds independently of the Reynolds number, even for fairly high values of this latter quantity. Since the effect of Re is mainly on the small scales, this suggests that mixing, in this two dimensional case, is controlled predominantly by the large coherent eddies. This is confirmed by inspection of the flow fields at high Re and Pe. The structure of the product is dominated by large folds and structures, with few small scales in the sense of fine random corrugations. This is also confirmed by

the relatively low values of the fractal dimension encountered. Several investigators have studied and measured the fractal dimensions of interfaces in *three dimensional* turbulence (Sreenivasan and Meneveau, 1988), arriving at $F \sim 7/3$, and have justified this value using models based on random homogeneous fractals. The same arguments when applied to two dimensional turbulence (Meneveau, private communication) result in $F = 2$. This is inconsistent with our observations.

The assumptions of randomness and homogeneity are not necessary for a fractal model. We have noted above that both the spirals generated by the deformation of initially plane interfaces by point vortices and the "stacks" resulting from the stretching those spirals by a plane strain are fractals. In fact, the stacks are both common in the two dimensional mixing interface and have a fractal dimension of 5/3, close to that observed in the layer after the first pairing. It is, therefore, tempting to conclude that they are the structures responsible for the fractal behavior of the interface in the two dimensional mixing layer and that the fractal transition observed at the pairing is caused by the straining of spirals formed by the original mixing eddies. A consequence of this interpretation is that, by inhibiting pairing altogether, we should be able to observe a transition to a lower fractal dimension of 4/3, and it can be argued that this is indeed the dimension implied by the product behavior in the case in figure 6 for which both pairings were inhibited. This case is, however, not representative of natural mixing layers and was not studied in great detail.

Note that this picture is very different from that of the wrinkled interface of a homogeneous fractal. The fractional dimension comes in this case from the accumulation of turns near the center of the spirals and from the accumulation of sheets in the central part of the stacks. Note also that this picture is very similar to that arising from the *tendril-whorl* mapping studied in (Khakar *et al.*, 1986).

Conclusions

In summary, we have shown that the scalar interfaces in a two dimensional plane mixing layer acquire fractal properties, we have measured their fractal dimensions, and we have related them to the Péclet number dependence of product generation in a fast binary, diffusion controlled, chemical reaction. We have also shown that those dimensions and the generation of product are fairly independent of Reynolds number (for $\Delta U \delta_\omega / \nu \leq 90\,000$), although they are strongly dependent on molecular diffusivity, suggesting that the mixing is mostly due to "chaotic advection" from the large scale eddies. This is probably different from the behavior of the three dimensional mixing layer, in which a substantial part of the mixing seems to be associated to longitudinal vorticity and small scales.

The fractal dimension undergoes a transition from low values, in the range $F \approx 1 - 1.3$ to $F \approx 5/3$, which coincides in time with the first pairing and which is inhibited when this pairing is inhibited. The effect of the second pairing is not as marked. We have presented a model for these dimensions in terms of non-random, non-homogeneous, fractal structures. The transition is then explained as the generation during pairing of strained spirals ("stacks"). Finally, up to the Re

and Pe quoted above, we found no further transition either in the mixing efficiency or in the structure of the vorticity field.

It is especially significant that a simple geometric quantity, that can easily be measured by geometric means on flow fields at some high but finite Reynolds or Péclet numbers can be related to a scaling behavior valid for arbitrarily high Pe. The question of the behavior of diffusion limited chemical reactions in the limit of vanishing diffusivity is an important unsolved problem for real *three dimensional* mixing layers. It is not known, for example, whether any reaction will occur in the limit $Pe \to \infty$, and experimental evidence is scarce and difficult to come by. If a relation similar to the one discovered here could be proved in that case, all that would be needed would be a measurement of the fractal dimension of the interface at some Péclet number high enough for a clear separation to exist between the Batchelor and outer scales of the flow. Some preliminary experiments with existing numerical flow fields show that the available Reynolds numbers do not satisfy this condition. The arguments in section 5, on the other hand, suggest that the usual estimates for the turbulent scales can be used to estimate the extent of the fractal range, if one exists, in which case the smallest fractal scale should decrease faster with Pe in the three dimensional case (where $W \sim Pe^{-3/4}$) than in the two dimensional one ($W \sim Pe^{-1/2}$). If this is so, a computation of a mixing flow with the appropriate Pe might be just within the capability of the next generation of computers, and that numerical experiment might provide a simple answer to the question of asymptotic product behavior in three dimensional layers.

The part of this work that was carried out in the University of Madrid was supported by United Technologies Corporation of Hartford, Conn.

REFERENCES

AREF, H. 1984 Stirring by chaotic advection. *J. Fluid Mech.* **143**, 1-21.

BREIDENTHAL, R. 1981 Structure in turbulent mixing layers and wakes, using a chemical reaction. *J. Fluid Mech.* **109**, 1-24.

JIMÉNEZ, J. 1983 A spanwise structure in the plane mixing layer. *J. Fluid Mech.*. **132**, 319-336.

JIMÉNEZ, J. & MARTEL, C. 1990 Fractal properties of interfaces in two dimensional shear layers, *Proc. IUTAM Symp. Stirring and Mixing.* La Jolla, 20-24 August, 1990.

KHAKHAR, D. V., RISING, H. & OTTINO, J. M. 1986 An analysis of chaotic mixing in two chaotic flows. *J. Fluid Mech.* **172**, 419-451.

KONRAD, J. H. 1977 An experimental investigation of mixing in two dimensional turbulent shear flows with applications to diffusion limited chemical reactions, *Ph.D. Thesis.* Caltech.

LESIEUR, M., STAQUET, C., LE ROY, P. & COMTE, P. 1988 The mixing layer and its coherence examined from the point of view of two dimensional turbulence. *J. Fluid Mech.* **192**, 511-534.

MANDELBROT, B. B. 1982 *The fractal geometry of nature.* W. H.Freeman.

MOSER,R. D. & ROGERS,M. M. 1990 Mixing transition and the cascade to small scales in a plane mixing layer, *Proc. IUTAM Symp. Stirring and Mixing.* La Jolla, 20-24 August, 1990.

SREENIVASAN, K. R. & MENEVEAU, C. 1986 The fractal facets of turbulence. *J. Fluid Mech.* **173**, 357-386.